

CHARACTERIZATION OF PLASTIC FLOW CURVES OF AUSTENITIC STAINLESS STEEL ISO 5832-9 USED IN ORTHOPEDIC APPLICATIONS

CARACTERIZAÇÃO DAS CURVAS DE ESCOAMENTO PLÁSTICO DO AÇO INOXIDÁVEL ISO 5832-9 USADO EM APLICAÇÕES ORTOPÉDICAS

E. S. Silva ^{(1)*}, O. Balancin ⁽¹⁾, R. C. Sousa ⁽²⁾ & J.M. Cabrera ⁽³⁾

(1) Universidade Federal de São Carlos, UFSCar. São Carlos, SP, Brasil. (2) Universidade Federal do Maranhão – UFMA. (3) Universitat Politècnica de Catalunya – UPC

Abstract

Austenitic stainless steels have been used as materials for orthopedic implants. Recent research has shown that steel ISO 5832-9 is an alternative for orthopedic applications involving severe loads and long residence time in the human body. This work is to characterize the plastic behavior of steel under conditions similar to industrial processing. The curves of plastic flow were obtained by torsion tests at different strain rate and temperature. The results show that the apparent activation energy is relatively high, and the reasons for tensions between critical peak and steady state. These high values suggest the mechanism of action of hardening with dynamic softening. It discusses the role of precipitation dynamics through mathematical analysis of the shape of the curve. Hardening in the region is evaluated several ways of increasing tension with the strain to peak stress. In the region of dynamic softening is used Avrami formalism to characterize the kinetics of recrystallization.

Key-words: Metallic biomaterials; Dynamic Recrystallization (DRX), Dynamic Precipitation, Phase Z (NbCrN), plastic instability.

Resumo

Os aços inoxidáveis austeníticos vêm sendo utilizados como materiais para implante ortopédico. Pesquisas recentes têm mostrado que o aço ISO 5832-9 é uma alternativa para aplicações ortopédicas que envolvem cargas severas e longos tempo de permanência no corpo humano. Neste trabalho, faz-se a caracterização do comportamento plástico desse aço em condições similares às do processamento industrial. As curvas de escoamento plástico foram obtidas através de ensaios de torção a diferente taxa de deformação e temperatura. Os resultados mostram que a energia de ativação aparente é relativamente alta, bem como as razões entre tensões críticas, pico e estado estacionário. Esses altos valores sugerem a atuação de mecanismo de endurecimento juntamente com amaciamento dinâmico. Discute-se o papel da precipitação dinâmica através da análise matemática da forma da curva. Na região de endurecimento são avaliadas as diversas formas de aumento da tensão com a deformação até o pico de tensão. Na região de amaciamento dinâmico utiliza-se o formalismo de Avrami para caracterização da cinética de recristalização.

Palavras-Chave: Biomateriais metálicos; Recristalização dinâmica (DRX), Fase Z (NbCrN)

1 Introduction

The use of stainless steel with high N has been studied and applied heavily over the past 20 years as biomaterials. Currently, the strong demands in orthopedic problems are found in bone joints and degenerative inflammatory conditions affecting millions of people around the world, reported by Ornhaugen (1996), Belyakov (1998) and Sakai (2004). The material currently used in the manufacture of orthopedic implants is the ASTM F138 (ISO 5832-1) which has compromised the mechanical properties and corrosion in the annealed condition, Giordani (2006). In addition to its high contents of Ni (> 12%) which according to the International Agency for Research on Cancer (IARC) of World Health Organization (WHO) are carcinogenic to the human body. To alleviate these problems steels with high content of N, Cr, Ni and low concentrations of Ni (steel ISO 5832-9) are being used in medical applications.

In general three phenomena control the appearance of the curves of plastic flow of materials: hardening characterized by heightened tension, dynamic recovery (DRV) is characterized by the saturation stress with increasing deformation and dynamic recrystallization (DRX) described by the peak stress (σ_p) curve of plastic flow, **Figure 1**, Poliak (1996), Diao (2007) and Mc. Queen (2002). But for complex compositions of materials likely to dynamic precipitation formation, or even coming from thermal treatment, this room can be a phenomenon that interacts with existing ones significantly changing the appearance of the curves of plastic flow and therefore the mechanical properties of the material, Mataya (1996).

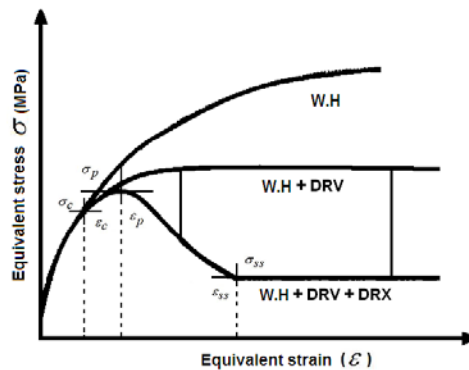


Figure 1 Three main mechanisms of hardening and softening in the hot torsion tests

2 Material and Methods

The ASTM F1586 (ISO 5832-9) was produced by Villares Metals S.A (Brazil) in the form of rolled bars with diameter of 20 mm in the annealed condition to 1030 °C for 60 minutes and cooled in water. This steel is a composition based 21Cr-10Ni-3, 6Mn-2, 4Mo with addition of 0.37 N. The curves of plastic flow of steel ISO 5832-9 were determined using isothermal hot torsion machine in a continuous horizontal in the laboratory of thermomechanical treatment DEMa / UFSCar (Brazil). The specimens were heated to a temperature of 1250 °C solubilization and maintained by 300s to complete homogenization, then cooled to the temperature of testing remain for 30s before undergoing deformation, which the strain rate ranged from 0.01 to 10 s⁻¹ in a temperature range of 900 to 1200 °C. Immediately after deformation, the specimens were tempered in water, followed by treatment with metallographic attack with an electrochemical solution of 65% HNO₃. The measure of the recrystallized grain size (d_{DRX}) was determined by linear intercept method.

The morphology of precipitates was made by scanning electron microscopy (SEM), model Zeiss Ultra Plus, along with a semiquantitative analysis of the composition with a microanalysis by dispersive X-ray (EDS), X-Max Oxford Instruments INCA software and, coupled with SEM, belonging to the Technological Centre of Manresa (CTM), Spain. To estimate the precipitates present in steel ISO 5832-9 is used software for calculation of phase diagram, Factsage 6.1, with integrated database on thermodynamic calculations.

3 Results

Description of the curves of plastic flow of steel ISO 5832-9 – Constitutive relations

Curve stress vs. stress, Figure 2 shows a typical behavior of materials that recrystallise dynamically with a simple peak stress followed by a gradual decrease with deformation subsequent to an intermediate value between the stress onset of plastic flow (σ_o) and peak stress (σ_p) and can or fail to reach the steady-state stress (σ_{ss}). Three well-defined stages are observed: hardening, softening and steady state: First, there is a region of work hardening (W.H). Then one attains a state of maximum stress corresponding to the peak in the curve. In those circumstances can see that the curves can be separated into three regions according to their peak deformation (ϵ_p). Finally a transitional stage of softening by deformation. It is observed that as a increases or decreases are apparently softened the curves beyond the peak. This phenomenon was also observed by Dehghan & Hodgson [8] to investigate the recrystallization of AISI 304.

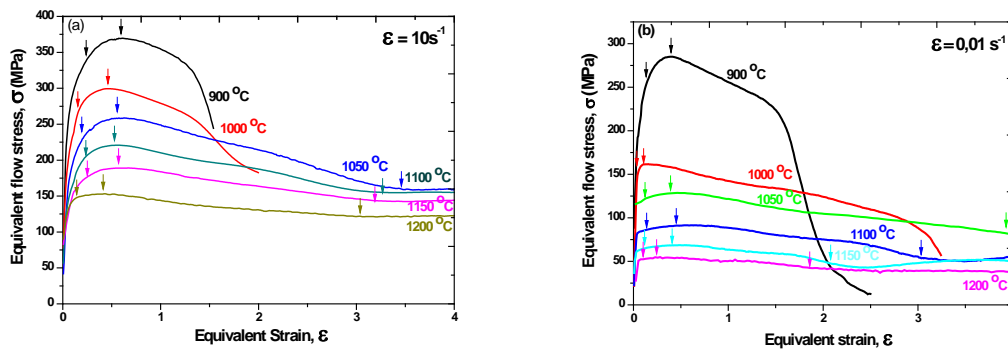


Figure 2 Curve σ vs. ϵ , isothermal continuous: (a) $\dot{\epsilon} = 10s^{-1}$; (b) $\dot{\epsilon} = 0,01s^{-1}$.

The onset of DRX, (σ_c, ϵ_c) was determined by analyzing the flow curves using the plastic work hardening rate (θ) as a function of equivalent stress (σ) using the method developed by N. D. Ryan & Mc. Queen and perfected by J. J. Jonas (2009), E. I. Poliak (1996) and A. Najarfizadeh (2006). In this method the onset of DRX is associated with the inflection point on the curve θ vs. σ . The relations between the stresses and strains show an average ratio of: $\sigma_c / \sigma_p = 0,91$, $\sigma_c / \sigma_{sat} = 0,87$, $\epsilon_c / \epsilon_p = 0,33$, $\sigma_p / \sigma_{ss} = 1,33$, $\sigma_c / \sigma_{ss} = 1,22$. Similar relationships are reported in the literature: Steel C - Mn ($\sigma_c / \sigma_p = 0,78$; $\epsilon_c / \epsilon_p = 0,50$), Nb Steel ($\sigma_c / \sigma_p = 0,85$; $\epsilon_c / \epsilon_p = 0,55$) and steel F-138 ($\sigma_c / \sigma_p = 0,89$; $\epsilon_c / \epsilon_p = 0,30$), Giordani (2006). These relationships for steel ISO 5832-9 show that they are independent of the variation $\dot{\epsilon}$, even with this change has significantly

influenced the critical strain (ϵ_c) for the DRX. To lower $\dot{\epsilon}$ the critical strain for DRX (ϵ_c) is lower, mainly high T .

Figure 3 shows the variation of peak stress (σ_p) with the strain rate ($\dot{\epsilon}$) for steel ISO 5832-9. The exponent of stress (slope, m) is not maintained constant increases continuously with temperature. The sensitivity to strain rate (m) and temperature vary with the deformation, ie, the density of disagreement varies. With increasing strain rate, the rate of dynamic recovery (DRV) decreases followed by an increase in critical stress (σ_c) and peak (σ_p). One effect was observed on the dependence of yield stress with plastic strain rate ($\dot{\epsilon}$) is the plastic instability that can lead an early stage of stretching of the material during the deformation process expressed by m affecting the onset of plastic instability that among other factors is affected by grain size, dislocations, temperature, processing routes etc.

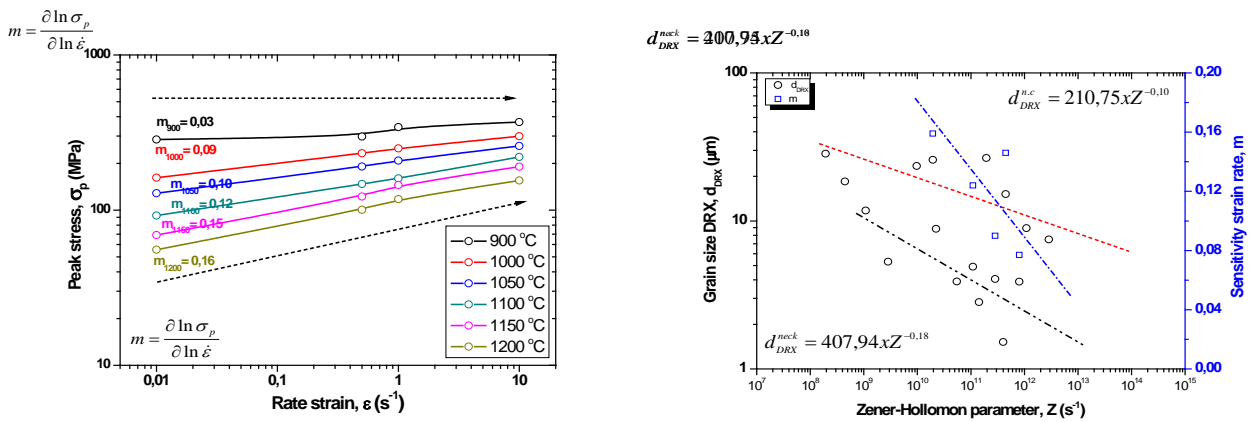


Figure 3 a) curve of peak stress (σ_p) vs. strain rate ($\dot{\epsilon}$). b) Dependence of the DRX grain size (d_{DRX}) and Z with sensitivity to strain rate (m).

Characterization of flow stress

The compensation effect of temperature on the deformation rate, considering the energy autodifusão for austenitic stainless steel ($Q_{SD} = 290kJ/mol$), through the formalism developed by Cabrera (1997), where the input variables are normalized by autodifusão coefficients $D(T)$ and Young's modulus $E(T)$, creep coefficient, $n = 5$ shows two remarkable behaviors, Figure 4a. The first refers to the regions of high T and low $\dot{\epsilon}$, where the experimental points reasonably fit a power function. A second region is characterized by having higher growth, whose exponential function expressed by hyperbolic sine respond satisfactorily to experimental data. Figure 4b shows how the ISO 5832-9 steel fits the classic relationship of Derby developed for various materials with a dispersive distribution of points with two distinct behavior resulting from interference in the kinetics of DRX as a product of the dynamic process of accumulation and annihilation of dislocations together with the interaction of particles with Z phase precipitates acting as hardening agent, reported by Mataya (1996) and Girdani (2005). This interaction interferes with the intensity of the stresses of steady state (σ_{ss}) and the recrystallized grain size (d_{DRX}).

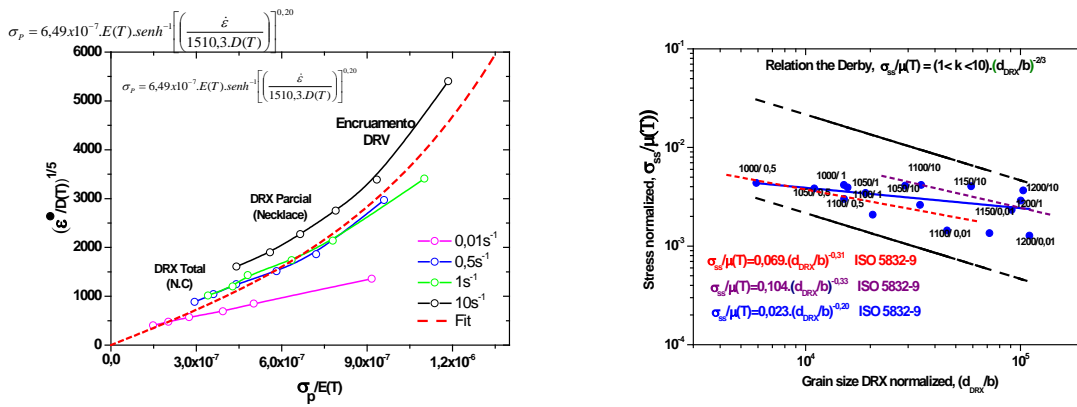


Figure 4 a) Representation of the peak stress (σ_p) as a function of processing parameters according to the law of the normalized hyperbolic sine; b) Relationship classic Derby, σ_{ss} and d_{DRV} .

Description of the phenomena of strain hardening, dynamic recovery and recrystallization

The DRV is a thermally activated process, with the coefficient of DRV (r) responsible for the softening and microstructural dependent deformation conditions (values Z). From the formalism developed by Jonas (2009) to the work hardening rate facing the stress of plastic flow was possible to determine the coefficients of strain hardening and dynamic recovery, DRV (r) steel ISO 5832-9. Figure 5 shows that r decreases with increasing peak stress (σ_p), corresponding to a decreased T and increased $\dot{\epsilon}$. The strain hardening coefficient (h) shows an inverse behavior.

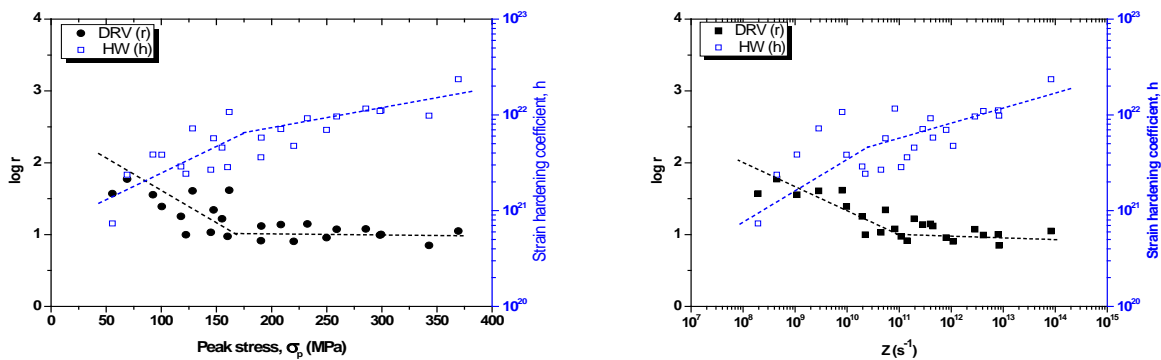


Figure 5 Dependence of strain hardening coefficient (h) and dynamic recovery, DRV (r) with the peak stress (σ_p) and Zener-Hollomon parameter, Z the curves of steel ISO 5832-9.

In the formalism J. J. Jonas Avrami exponent (n) is of great importance for understanding the kinetics of DRX during the whole deformation process, not only in peak condition, revealing characteristics of the kinetics of nucleation, growth and possibly the interaction of precipitation dynamics. From the simulation curve recovered was possible to estimate the fractional softening and hence determine n under various conditions of deformation, Figure 6. Observe that the value of Avrami exponent (n) decreases with the progress of recrystallization. The dependence of the Avrami exponent (n) with the parameter Z show a decrease n with the increase of Z . For low values Z , n seems high, $n \sim 3$. However, for moderate values of Z the value n is reduced, $n \sim 1,2$.

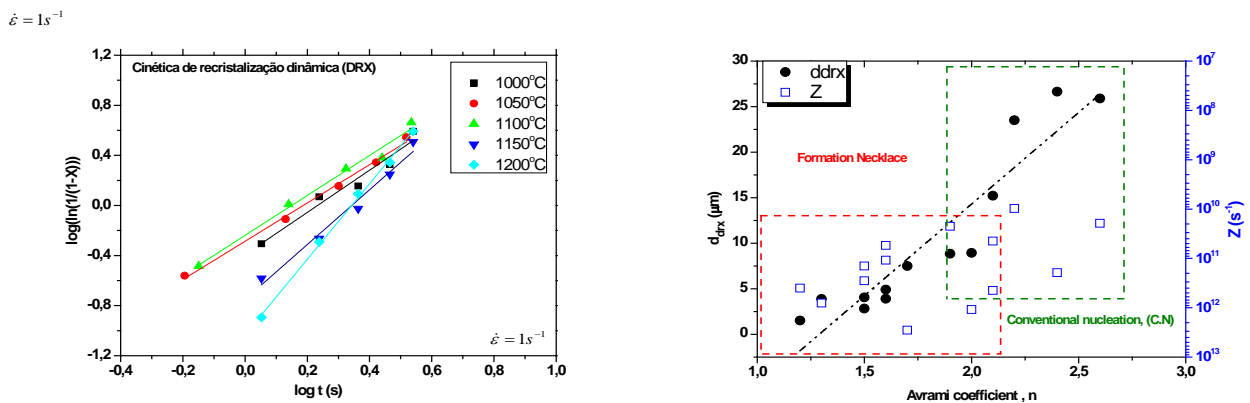


Figure 6 a) Avrami curve for steel to ISO 5832-9 1050 °C - $1s^{-1}$. b) Behavior and Zener-Hollomon parameter (Z) compared to the Avrami exponent, (n).

Microstructural analysis of austenitic stainless steel ISO 5832-9

The microstructures of steel ISO 5832-9 under different processing conditions allow to classify the microstructural phenomena in three regions according to the values of Zener-Hollomon parameter (Z): **Region I**: high values Z (T low and $\dot{\epsilon}$ high, $Z_{max} \sim 10^{14}$) where we observe a predominance mechanisms of hardening and dynamic recovery (DRV), characterized by an elongated grain structure with no evidence of recrystallization, Figure 7. **Region II**: presents moderate values Z (balance between T and $\dot{\epsilon}$, $Z_{med} \sim 10^{11}$). This region covers temperatures between 1000 and 1150 °C with strain rates of 0.01 to $10s^{-1}$ in this region the structure is striking necklace with dynamic recrystallization (DRX) developing in partial and heterogeneously. **Region III**: Lower values Z (high T and low $\dot{\epsilon}$, $Z_{min} \sim 10^8$) the kinetics of DRX is accelerated and the formation of necklace is not as obvious as for moderate Z conditions. In this case the nucleation of new grains deformed DRX starts very low and the mobility of grain boundaries is high and separate serrated rapidly evolving in the region (conventional nucleation, C.N).

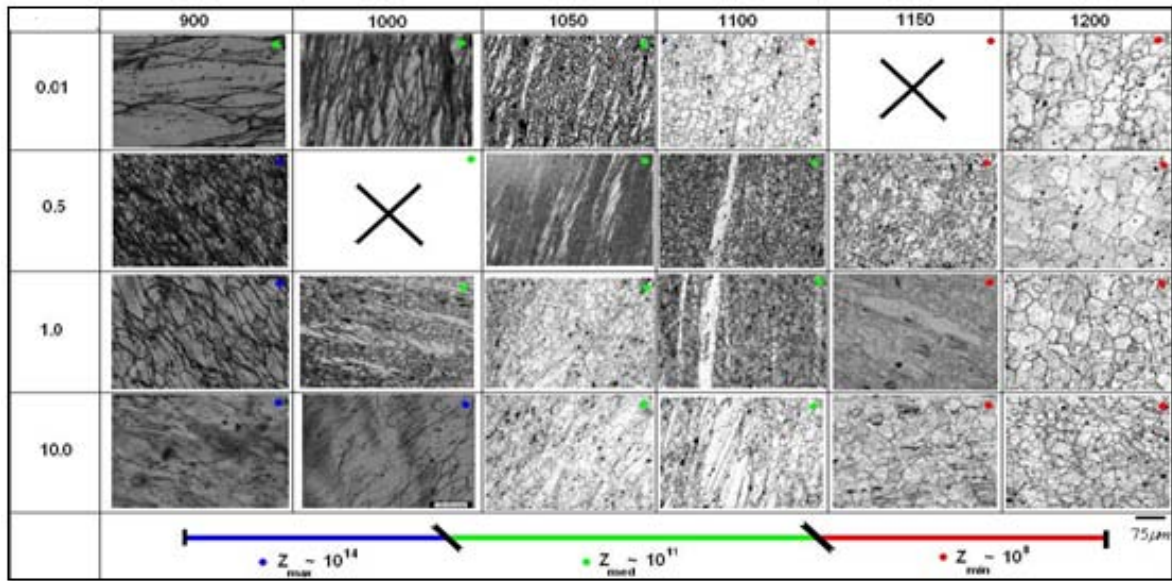


Figure 7 Appearance microstructural ISO 5832-9 steel torsion test under isothermal continuous.

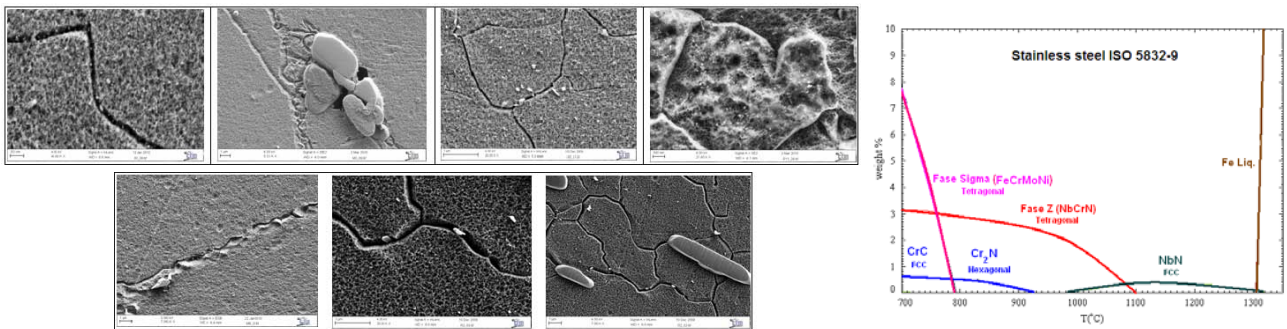


Figure 8 a) Particles precipitated from Phase Z (NbCrN) interacting with the matrix and the contours of the new DRX grains b) Calculation of steel Factasage 6.1 of ISO 5832-9.

Discussion

This typical dynamically recrystallized material due to generation of dislocations, crystal twinning and deformation bands when the material is deformed by heating. The increase of dislocations leads to an increase in the strength of the material through the accumulation and interaction with the dislocations totally randomly tangled and far from each other by reducing the mobility of the same [8,15]. In materials with high stacking fault energy ($SFE > 90 \text{ mJ/ m}^2$), the climbing and sliding cross DRV make more effective when compared with materials with low and medium SFE ($10 < SFE < 90 \text{ mJ/ m}^2$), Cabrera (1997). The ISO 5832-9 steel presents a SFE around 68.7 mJ/ m^2 , Girodani (2006) considered the average SFE with annihilation rate of discrepancy generally smaller than the generation rate due to low efficiency of thermally activated mechanisms. As a consequence there is an accumulation of dislocations leading to a heterogeneous distribution favoring the nucleation of new grains DRX, Dehghan (2008). This high value on reason $\sigma_c / \sigma_p = 0,91$ is justified by the high stress levels necessary for the occurrence of DRX in the wake of increase in the density of dislocation intensifying the work hardening thereby causing a marked rise for the high activation energy. Another contribution is the presence of particles of precipitates formed during hot deformation, and / or disposal of nitrogen (N), chromium (Cr) and niobium (Nb) solid solution by increasing the frictional stress of the crystal lattice, reflecting directly on the yield strength of the material decrease in SFE, generating a significant increase in efficiency of grain boundaries as obstacles to the movement of dislocations such that the critical strain for DRX is high compared with other materials, Najafizadeh (2006).

The variance in the exponent of the stress (m) suggests that the behavior of steel ISO 5832-9 cannot be described by simple equations of power law. The sensitivity to strain rate (m) is variable as a result of the density mismatch and the presence of precipitated particles of Z phase interacting strongly with the dislocations and new DRX grains. The value m reflects the activity of the grain boundary to the plasticity of the material leading to a thermally activated relaxation of the grain boundary. A low value for m ($m = 0,03$) with low DRV provides a limited ductility justified by the propensity for plastic instability manifesting with stretch material with plastic instability and severe stage of plastic deformation and stable short allowing a little space to maintain a behavior deformation and σ becomes practically independent of $\dot{\epsilon}$, Figure 3a. With the increase of m ($m = 0,16$), the plastic instability is enhanced by generating finer grains. The dynamically recrystallized grain size (d_{DRX}) is smaller the lower the value of m whose evolution influences the behavior of plastic deformation and grain refinement. Resistance is attributed among other reasons the increasing fraction of the grain boundary, dislocation and stacking of particles precipitated. But the affection of the dislocations is not the main reason for the development of sensitivity to strain rate (m), but the increasing fraction of the grain boundary because with increasing volume fraction of grain boundary for d_{DRX} a small amount to contribute the activity of the grain boundary during deformation causing the stress is more sensitive to strain rate.

Curves of plastic flow is observed that some points are far outside the trend line given by the hyperbolic sine law that overestimates the stress values found for low T and high $\dot{\epsilon}$. These points will describe a balance T and $\dot{\epsilon}$ on the kinetics of recrystallization and precipitation of steel ISO 5832-9, reflecting the appearance of the curve. These values are overestimated and those points coming off the trend are justified by the predominance of work hardening on the DRV in the early part of the curve and the presence of particles of precipitated phase Z that are generated dynamically interacting with the dislocations and new DRX grains inhibiting and controlling the kinetics of nucleation and grain growth. Consequently these two contributions help to increase the mechanical strength of the material generating a tougher microstructure with finer grain size.

The reduction in the coefficient of DRV (r) with increasing peak stress (σ_p) is physically reasonable since the DRV rate tends to increase with the increase T and decrease $\dot{\epsilon}$ resulting in a balance of work hardening, DRV and DRX early. Therefore it is observed that the material hardens quickly has a softening kinetics of microstructure and mechanical accelerated. At intermediate temperatures the coefficient of DRV (r) is strongly assisted by the softening of strain, governed by the landslide of dislocation by the deformation applied. The strain hardening coefficient (h) shows an inverse behavior reflecting the mean free path of dislocations (distance traveled by a segment of dislocation before it is stored by interaction with the microstructure) [6] and is dependent on the dislocation density (interaction and orientation), grain size and particle precipitates with the heterogeneity of dislocations changing the process of hardening at the beginning of the curve. So the hardening curve at the beginning of plastic flow is not a stage but a mechanism governed by the relationship between the mean free path and the length of the dislocations with the critical distance for annihilation of dislocations (contributing DRV) is not a sequence based on temperature fusion or diffusion coefficient, but the SFE, Derby (1992).

The DRV coefficient (r) decreases with increasing Z speed since most of the DRV process takes place for low Z . Moreover, for high values Z , where the diffusion mechanisms are less influential, speeds tend to be softening constant, Figure 5. So the DRV is heavily dependent on T and gently to $\dot{\epsilon}$ and not depend directly on time. The dependence of strain hardening coefficient (h) shows up to converse with a growing due to the presence of twinned, whose contours help to increase by immobilizing the mean free path of dislocations, Najafizadeh (2006). Additionally the effect of small precipitates of phase Z (NbCrN) interacting with each other and dislocations influence the appearance of curves. The decrease h with deformation and is strongly dependent on T the low $\dot{\epsilon}$, indicating the need for a yield stress more intense with higher activation energy. Then to top Z if the hardening prevails over the DRV and the microstructure develops heterogeneously.

The low value of Avrami exponent (n) takes place because of the heterogeneity in the process of DRX. Another reason is the delay and prolongation of the process of DRX due to the presence of precipitated particles of phase Z . As for the Zener-Hollomon parameter (Z) observe that there is a decrease n with the addition of Z predominant nucleation at grain boundaries and twinned (conventional nucleation, C.N). In this condition the rate of nucleation is relatively high, where the new DRX grains finished their growth through collision between them. In the region of moderate values of Z the DRX is controlled by nucleation of new DRX grains and particles of phase Z with the relatively low number of nucleation sites with low values of n ($n=1,2$) and growth is controlled by a large number of cores on growth that collide with each other and the precipitates mutually limiting the mobility of the contours of the new grain formation necklace.

The estimate of precipitates present in the steel using the ISO 5832-9 Factsage 6.1, Figure 8 predicts the formation of five types of compounds: Phase Z (NbCrN), NbN, Cr₂N, Cr₂₃C₆, Phase σ (FeCrMoNi). At high temperatures the precipitates that prevail are the most stable, such as the Z phase and the NbN that interact with the new DRX grains interfering with the kinetics of DRX. The presence of these precipitates was analyzed by SEM / EDS, Figure 7. The chemical composition of Z phase showed an atomic percentage of: 50.33% Nb, 35.42% Cr, 6.37% N, bal. Fe These values are in agreement for materials of similar composition obtained by Ornhaugen (1996) and Giordani (2005). It should be emphasized that the calculation by FactSage considers situations in balance so that this material is under various thermodynamic and kinetic changes of different thermomechanical processing conditions.

Conclusions

- The plastic flow curves show high values between the strains, $\sigma_c / \sigma_p = 0,91$, indicating that the onset of DRX (σ_c) is being slowed by the high rate of hardening precipitates and particles of the Z stage which anchor the grain boundaries and the mobility of dislocations;
- The instability of plastic steel ISO 5832-9 as expressed by the sensitivity to strain rate (m) shows the activity of the grain boundary to the plasticity of the material leading to a thermally activated relaxation of the grain boundary.
- The correlation of microstructural and mechanical steel ISO 5832-9 second values of: (i) High Z (low T and high $\dot{\epsilon}$) are predominant mechanisms of work hardening and DRV, characterized by an elongated grain structure in the form of pancakes, with no evidence of recrystallization (ii) Moderate Z (balance T and $\dot{\epsilon}$) the formation of the necklace structure is marked with the DRX and developing in part influenced by the presence of heterogeneously precipitated phase Z (NbCrN), (iii) Low Z (high T and low $\dot{\epsilon}$), where the kinetics of DRX is accelerated and the formation of necklace is not so obvious, featuring conventional nucleation (C.N), DRX total;
- The Avrami formalism showed values for n steel ISO 5832-9, between 1.2 to 3.0 with a predominance of nucleation on crystal twinning, contours and surfaces of the grains. The low value corresponding to the formation of necklace and high values of n one has the conventional nucleação;

Acknowledgments

To CAPES for financial support. Groups to search UFSCar (Brazil) and UPC (Spain) coordinated by Professors Alberto M. Junior and Jose M. Cabrera. ☒

Bibliographical references

- 1 Belyakov, A. Miura, H., Sakai, T. Mater. Sci. Eng. A 255 (1998) 139–147.
- 2 Cabrera, J.M., Omar, A. A., Jonas, J.J., Prado, J.M., Metall. Mater. Trans. A28 (1997) 2233.
- 3 Dehghan, M., Barnett, M.R. Materials Science and Engineering A, 485 (2008) 644-672.
- 4 Derby, B.: *Scripta Metall. Mater.*, 1992, vol. 27, pp. 1581-86.
- 5 Diao, Z.Y., Luo, H.W. Constitutive Analysis of Stress-Strain Curves of a High-Nitrogen Austenitic Stainless Steel. Proceedings of Sino-Swedish Structural Materials Symposium (2007).
- 6 Giordani, E.J., Jorge, A.M., Balancin, O. Scripta Materialia, 55 (2006) 743 - 746.
- 7 Giordani, E.J. Jorge Jr., A.M. Mater. Sci Forum, 500-501 (2005) 179.
- 8 Jonas, J.J., Quelennec, X., Acta Materialia 57 (2009) 2748–2756
- 9 Mataya, M.C., Perkins, C.A., Flow stress and microstructural evolution during hot working of alloy 22CR-13Ni-5Mn-0,3N ASS. Metal and Mater. Trans. A, volume 27A, 1996, 1251.
- 10 Mcqueen, H.J. Constitutive analysis in hot working. Mat. Sci. Eng. A322, 43-63, 2002.
- 11 Miura, H. T. Sakai, Hamji, H. Jonas, J.J. Scripta Mater. 50 (2004) 65–69.
- 12 Najafizadeh, A., Jonas, J.J. ISIJ International, 46 (2006) 1679-1684.
- 13 Örnham, C. Nilsson, J.O., Vannevik, H. Journal of Biomedical Materials Research, 31 (1996)
- 14 Poliak E.I., Jonas, J.J. Acta Mater., 1996;44:127.
- 15 Stewart, G.R., Jonas, J.J. ISIJ International 44 (2004) 1581–1589.

Corresponding authors: Santos, E.S. (edenshenc@yahoo.com.br) / Balancin, O. (balancin@power.ufscar.br)